

Minimum Energy Trap States of Dual-Spin Spacecraft

Michael G. Hollars*

Jet Propulsion Laboratory, California Institute of Technology, Pasadena, Calif.

The spin bearing assembly on a dual-spin spacecraft can encounter undesirable dynamic torques which exceed the available spin bearing motor torque, resulting in a failure to despin the stator (hence a "trap state"). This trap state torque is caused by static imbalance, dynamic imbalance, and asymmetry on the rotor and the stator, and is also a function of the rotational kinetic energy of the system. A general solution for the trap state torque is presented for dual-spin spacecraft at or near the minimum kinetic energy state. This covers all oblate dual-spin spacecraft near the all-spin mode with nutation damped out. The trap state torque equation for the case of small static and dynamic imbalances and asymmetries shows that the torque is primarily due to coupling between static imbalances or to coupling between dynamic imbalances on both bodies, but not to cross-coupling between static imbalance, dynamic imbalance, and asymmetry. The trap state torque equation extended to include large asymmetry on one of the bodies has an additional term due to cross-coupling between the large asymmetry on one body and dynamic imbalance on the opposing body. Design equations for the NASA/JPL Jupiter orbiter spacecraft Galileo are developed for sizing of the spin bearing motor and for mass property constraints.

Nomenclature

a, b	= maximum allowable center of mass offsets for Galileo stator and rotor, respectively	K	= rotational kinetic energy of spacecraft
a_0, a_1, a_2	= coefficients of eigenvalue equation	K_m	= minimum rotational kinetic energy of spacecraft for a given angular momentum
C_1, C_2, C_s	= centers of mass of bodies 1 and 2 and the total spacecraft, respectively	m	= $m_1 m_2 / (m_1 + m_2)$ = reduced mass
D_{xz1}	= $I_{xz1} + \epsilon_{x1} m r$ = component of dynamic imbalance of body 1 about the bearing axis	m_1, m_2	= mass of bodies 1 and 2, respectively
D_{yz1}	= $I_{yz1} + \epsilon_{y1} m r$ = component of dynamic imbalance of body 1 about the bearing axis	Q	= static imbalance term in the bearing torque equations
D_{xz2}	= $I_{xz2} - \epsilon_{x2} m r$ = component of dynamic imbalance of body 2 about the bearing axis	Q_{\max}	= maximum Q for a given set of spacecraft design constraints
D_{yz2}	= $I_{yz2} - \epsilon_{y2} m r$ = component of dynamic imbalance of body 2 about the bearing axis	R	= dynamic imbalance term in the bearing torque equations
H	= angular momentum of spacecraft	r	= distance separating the centers of mass of the bodies along the bearing axis
$[I]_1$	= centroidal inertia tensor of body 1 in coordinate frame $x_1 y_1 z_1$ with principal moments of inertia $I_{xx1}, I_{yy1}, I_{zz1}$ and products of inertia $I_{xy1}, I_{xz1}, I_{yz1}$	S_1	= $\sqrt{\Delta J_1^2 + I_{xy1}^2}$ = body 1 asymmetry
$[I]_2$	= centroidal inertia tensor of body 2 in coordinate frame $x_2 y_2 z_2$ with principal moments of inertia $I_{xx2}, I_{yy2}, I_{zz2}$ and products of inertia $I_{xy2}, I_{xz2}, I_{yz2}$	S_2	= $\sqrt{\Delta J_2^2 + I_{xy2}^2}$ = body 2 asymmetry
$[I]_s$	= centroidal inertia tensor of the complete spacecraft in coordinate frame $x_s y_s z_s$ with principal moments of inertia $I_{xxs}, I_{yyS}, I_{zzS}$ and products of inertia $I_{xyS}, I_{xzS}, I_{yzS}$	T	= dynamic bearing torque
J_t	= $\frac{1}{2} (I_{xx1} + I_{yy1}) + \frac{1}{2} (I_{xx2} + I_{yy2}) + m r^2$; for small center of mass offsets, ϵ , this is approximately the average transverse moment of inertia of the spacecraft about its center of mass	T_{\max}	= maximum dynamic bearing torque
J_z	= $I_{zz1} + I_{zz2}$; for small center of mass offsets, ϵ , this is approximately the moment of inertia of the spacecraft about the bearing axis	$x_1 y_1 z_1$	= body-fixed, mass-centered orthogonal coordinate frame of body 1
ΔJ_1	= $\frac{1}{2} (I_{xx1} - I_{yy1})$ = averaged difference between body 1 transverse moments of inertia = a component of body 1 asymmetry	$x_2 y_2 z_2$	= body-fixed, mass-centered orthogonal coordinate frame of body 2
ΔJ_2	= $\frac{1}{2} (I_{xx2} - I_{yy2})$ = averaged difference between body 2 transverse moments of inertia = a component of body 2 asymmetry	$x_s y_s z_s$	= mass-centered orthogonal coordinate frame of the spacecraft, fixed with respect to body 1
		α	= relative angular position between bodies 1 and 2 about the bearing axis
		$\epsilon_{x1}, \epsilon_{y1}$	= components of center of mass offset of body 1 from the bearing axis
		$\epsilon_{x2}, \epsilon_{y2}$	= components of center of mass offset of body 2 from the bearing axis
		$\epsilon_{xs}, \epsilon_{ys}$	= components of center of mass offset of the spacecraft from the bearing axis
		θ_1, θ_2	= phase shift angle between the x axis and a principal axis of transverse moment of inertia for bodies 1 and 2, respectively
		Λ_s	= spacecraft centroidal principal moment of maximum inertia
		λ	= eigenvalue
		Ω	= nominal spin rate of the spacecraft about the bearing axis

Introduction

A MINIMUM energy trap state occurs in a dual-spin spacecraft when the stator cannot be despun. The bearing axis motor generates insufficient torque to overcome dynamically generated bearing torque during the attempted

Presented as Paper 80-1780 at the AIAA Guidance and Control Conference, Danvers, Mass., Aug. 11-13, 1980; submitted Oct. 24, 1980. Copyright © American Institute of Aeronautics and Astronautics, Inc., 1980. All rights reserved.

*Engineer, Guidance and Control Section. Member AIAA.

stator despin maneuver. The dynamic bearing torque is generated by static imbalance, dynamic imbalance, and asymmetry on both bodies of the dual-spin system. In contrast, the bearing torque can also become a problem when it is desired to hold the stator fixed with respect to the rotor during certain spacecraft maneuvers. If the maneuver produces large changes in the spacecraft's mass property imbalances and asymmetries, the dynamic bearing torque may exceed the combined motor and friction torques and wrench the stator from its desired position.

Previous studies of the minimum energy trap state problem typically used simplified dual-spin spacecraft models to demonstrate the existence and character of the minimum energy trap state. Scher and Farrenkopf¹ analyzed a statically balanced model with dynamic imbalance on the stator and asymmetry on the rotor. Adams² analyzed a similar model with asymmetry added to the stator. This paper extends their work to the general solution including static imbalance, dynamic imbalance, and asymmetry on both the rotor and stator. The results of this analysis are applied to the dual-spin spacecraft Galileo, a Jupiter orbiter spacecraft to be launched in 1985 by NASA JPL to study the planet, its satellites, and local Jovian space.

Spacecraft Model

A general model of a dual-spin spacecraft is shown in Fig. 1. The model consists of two connected rigid bodies which can rotate relative to each other only about a single common bearing axis. As shown in the figure, there are three sets of coordinate axes defined. Axes x_1 , y_1 , and z_1 form an orthogonal triad, located and fixed at the center of mass of body 1, C_1 . Axis z_1 lies parallel to the bearing axis. The x_2 , y_2 , and z_2 axes are defined similarly for body 2. The orthogonal system axes x_s , y_s , and z_s are located at the system center of mass, C_s , but are parallel to axes x_1 , y_1 , and z_1 . Thus axis z_s also lies parallel to the bearing axis. The relative angle between the bodies, α , is defined to be the counterclockwise angular displacement of the x_2 axis with respect to the x_1 axis as viewed from the $+z$ direction.

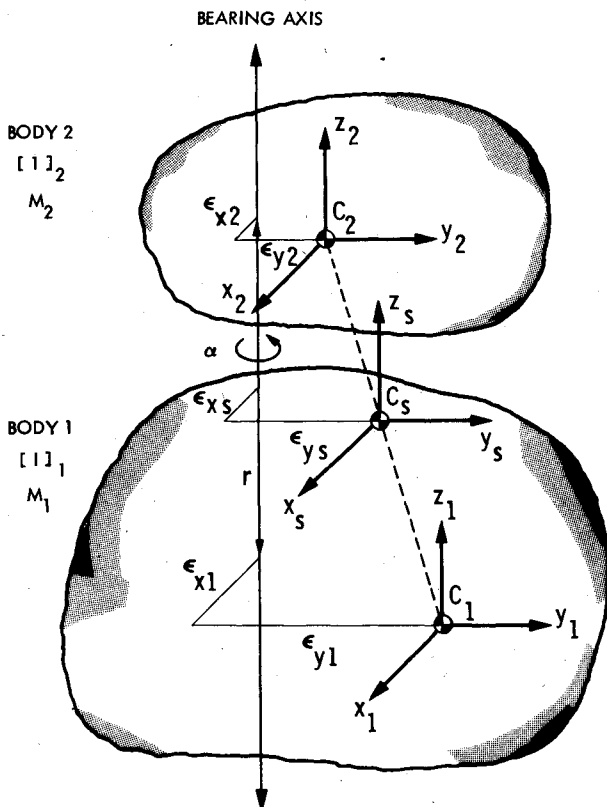


Fig. 1 Spacecraft model.

The center of mass offsets from the bearing axis, ϵ_x and ϵ_y , are measured in the xy plane of each body along the x and y axes, respectively. The centers of mass of the bodies are separated along the bearing axis by distance r . The centroidal inertia tensor of each body is designated by $[I]$, and the mass by m . The general solution of the dynamic bearing torque requires only that the spacecraft be an oblate dual-spinner. The only restrictions subsequently placed upon the model are that asymmetry, static imbalance, and dynamic imbalance are small ($\leq 10\%$), compared to the principal moments of inertia of each body. Subsequently, large asymmetry is allowed on one of the bodies. Thus, any reasonable combination of asymmetry, static imbalance, and dynamic imbalance can be represented by this model.

The centroidal inertia tensor $[I]_S$ of the rigid two-body dual-spin system can be derived in terms of the inertia tensors of the two bodies $[I]_1$ and $[I]_2$, and the geometry of the spacecraft. $[I]_S$ is required for analysis in the next section. The components of $[I]_S$ are derived using tensor rotation transformations and the parallel axis theorem. Each component is expanded in terms of principle inertias, geometry, static imbalances, dynamic imbalances, and asymmetries about the bearing axis (see Nomenclature):

$$I_{xxS} = J_1 + \Delta J_1 + \Delta J_2 \cos 2\alpha - I_{xy2} \sin 2\alpha + m(\epsilon_{y2}^2 \cos^2 \alpha + \epsilon_{x2}^2 \sin^2 \alpha - 2\epsilon_{y1}\epsilon_{y2} \cos \alpha + \epsilon_{x2}\epsilon_{y2} \sin 2\alpha - 2\epsilon_{x2}\epsilon_{y1} \sin \alpha + \epsilon_{y1}^2) \quad (1)$$

$$I_{yyS} = J_1 - \Delta J_1 - \Delta J_2 \cos 2\alpha + I_{xy2} \sin 2\alpha + m(\epsilon_{y2}^2 \sin^2 \alpha + \epsilon_{x2}^2 \cos^2 \alpha - 2\epsilon_{x1}\epsilon_{x2} \cos \alpha - \epsilon_{x2}\epsilon_{y2} \sin 2\alpha + 2\epsilon_{x1}\epsilon_{y2} \sin \alpha + \epsilon_{x1}^2) \quad (2)$$

$$I_{zzS} = J_z + m[\epsilon_{x1}^2 + \epsilon_{y1}^2 + \epsilon_{x2}^2 + \epsilon_{y2}^2 + 2(\epsilon_{x1}\epsilon_{y2} - \epsilon_{x2}\epsilon_{y1}) \sin \alpha - 2(\epsilon_{y1}\epsilon_{y2} + \epsilon_{x1}\epsilon_{x2}) \cos \alpha] \quad (3)$$

$$I_{xyS} = I_{xy1} + I_{xy2} \cos 2\alpha + \Delta J_2 \sin 2\alpha + m[\frac{1}{2}(\epsilon_{y2}^2 - \epsilon_{x2}^2) \sin 2\alpha + (\epsilon_{x1}\epsilon_{x2} - \epsilon_{y1}\epsilon_{y2}) \sin \alpha + (\epsilon_{x1}\epsilon_{y2} + \epsilon_{x2}\epsilon_{y1}) \cos \alpha - \epsilon_{x2}\epsilon_{y2} \cos 2\alpha - \epsilon_{x1}\epsilon_{y1}] \quad (4)$$

$$I_{yzS} = D_{yz2} \cos \alpha + D_{xz2} \sin \alpha + D_{yz1} \quad (5)$$

$$I_{xzS} = -D_{yz2} \sin \alpha + D_{xz2} \cos \alpha + D_{xz1} \quad (6)$$

Minimum Energy Trap

The kinetic energy of a damped spinning system will eventually reach a local minimum compatible with the system's angular momentum. Pringle³ demonstrated that this minimum energy state for a quasirigid body is one of spin about the body's centroidal principal axis of maximum inertia. To apply this result to a dual-spin system, viscous friction acts about the bearing axis until relative motion between the two bodies is stopped and, thus, can be considered quasirigid. The minimum kinetic energy of the dual-spin system in this state is given by

$$K_m(\alpha) = |H|^2 / 2\Lambda_S(\alpha) \quad (7)$$

where the angular momentum H is constant (no external torques applied) and the spacecraft maximum centroidal principal moment of inertia Λ_S is a function of spacecraft mass properties and geometry which varies with α . Λ_S , the largest eigenvalue of $[I]_S$, is found by solving for the largest root of the eigenvalue equation

$$|[I]_S - \lambda I| = \lambda^3 + a_2 \lambda^2 + a_1 \lambda + a_0 = 0 \quad (8)$$

where

$$a_0 = I_{xyS}^2 I_{zzS} + I_{yzS}^2 I_{xxS} + I_{xzS}^2 I_{yyS} - 2I_{xyS} I_{yzS} I_{xzS} - I_{xxS} I_{yyS} I_{zzS} \quad (9)$$

$$a_1 = I_{xxS} I_{yyS} + I_{yyS} I_{zzS} + I_{xxS} I_{zzS} - I_{xyS}^2 - I_{yzS}^2 - I_{xzS}^2 \quad (10)$$

$$a_2 = -I_{xxS} - I_{yyS} - I_{zzS} \quad (11)$$

The components of $[I]_S$ are listed in Eqs. (1-6). For the Galileo mass properties and geometry listed under case A in Table 1, the minimum kinetic energy as a function of α is plotted in Fig. 2 as a solid line. The local minimum on the plot indicates the value of α to which the system will settle if only viscous friction acts about the bearing axis. Maximum K_m is a point of unstable equilibrium.

Table 1 Galileo worst-case mass properties

Symbol	Case A	Case B	Case C	Units
J_1	4583.7	4583.7	4300.0	kg-m ²
J_z	5750.0	5750.0	5695.0	kg-m ²
ΔJ_1	155.0	155.0	300.0	kg-m ²
I_{xy1}	10.0	10.0	40.0	kg-m ²
S_1	155.3	155.3	303.0	kg-m ²
ΔJ_2	50.0	50.0	40.0	kg-m ²
I_{xy2}	50.0	50.0	40.0	kg-m ²
S_2	70.7	70.7	56.6	kg-m ²
D_{xz1}	20.0	20.0	60.6	kg-m ²
D_{yz1}	20.0	20.0	60.6	kg-m ²
D_{xz2}	0.1	0.1	19.4	kg-m ²
D_{yz2}	0.1	45.0	19.4	kg-m ²
a	0.0254	0.0254	0.0350	m
ϵ_{x1}	0.0180	0.0180	0.0250	m
ϵ_{y1}	0.0180	0.0180	0.0250	m
b	0.0350	0.0350	0.0350	m
ϵ_{x2}	0.0250	0.0250	0.0250	m
ϵ_{y2}	0.0250	0.0250	0.0250	m
m	615.0	615.0	589.0	kg
m_1	988.0	988.0	950.0	kg
m_2	1630.0	1630.0	1550.0	kg
r	1.50	1.50	1.40	m
Ω	1.0472	1.0472	1.0472	rad/s

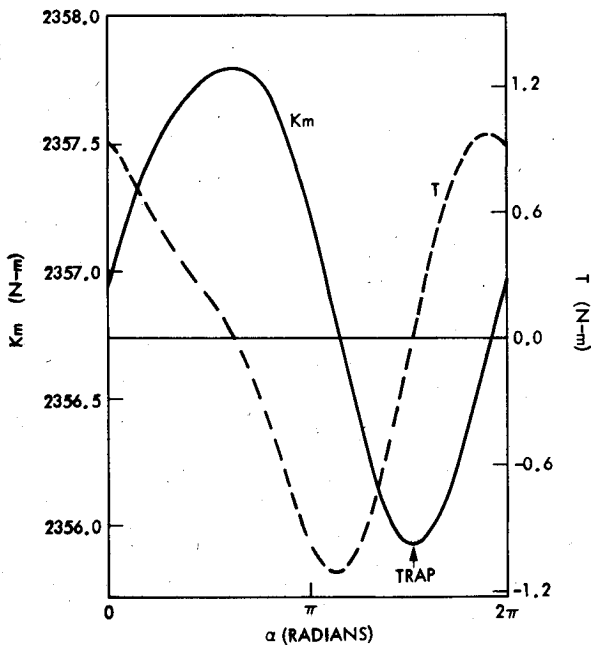


Fig. 2 Minimum kinetic energy and bearing torques as a function of α .

Scher and Farrenkopf¹ estimated the upper limit motor torque required to escape the minimum energy trap as the torque required to hold the two bodies fixed with respect to each other for any value of α . Deriving Lagrange's equation of motion for the rigid two-body, dual-spin spacecraft model and applying the holonomic constraint $\dot{\alpha} = 0$, yields the torque equation

$$T = -\partial K / \partial \alpha \quad (12)$$

Applying this equation to the minimum energy state of the spacecraft and expanding yields

$$T = -\frac{\partial K_m}{\partial \alpha} = -\frac{\partial K_m}{\partial \Lambda_S} \frac{\partial \Lambda_S}{\partial \alpha} \quad (13)$$

which can be implicitly evaluated from Eqs. (7) and (8) as

$$T = \frac{1}{2} |H/\Lambda_S|^2 \times \left\{ \frac{\Lambda_S^2 (da_2/d\alpha) + \Lambda_S (da_1/d\alpha) + (da_0/d\alpha)}{3\Lambda_S^2 + 2a_2\Lambda_S + a_1} \right\} \quad (14)$$

Direct evaluation of this torque equation, using the spacecraft inertia tensor components, yields over 1000 terms. The computer-assisted algebra software package MACSYMA (see Acknowledgments) analytically evaluated this general torque equation. The dotted line in Fig. 2 is a plot of T for the Galileo mass properties listed under case A in Table 1. Note that there are two points at which $T=0$ for this set of mass properties. The crossing at $\alpha \approx 3\pi/2$ is a minimum energy trap. The crossing at $\alpha \approx 2\pi/3$ is a point of unstable equilibrium. Other spacecraft mass properties can generate multiple maxima and minima. The next section describes an order analysis in which third-order and higher terms are dropped for special cases.

Reduced Order Analyses of Bearing Torque

Although the exact solution of dynamic bearing torque for the general case was determined, physical interpretation of the results was hampered by the huge size of the equation. Consequently, the general bearing torque Eq. (14) was evaluated for the special case of small static imbalance, small dynamic imbalance, and small asymmetry on both bodies. Center of mass offsets, asymmetry, and products of inertia are considered to be first-order variables. The principal moments of inertia, center of mass separation distance r , and the reduced mass m are considered to be zeroth-order variables. For the Galileo dual-spin spacecraft (Table 1), this analysis allows center of mass offsets of up to 10 cm, products of inertia and asymmetries of up to 300 kg-m² in the rotor and 30 kg-m² in the stator. Note, however, that the Galileo stator has much larger asymmetry than allowed for in this analysis. Large asymmetry for one body will be analyzed at the end of this section.

MACSYMA was used to perform the reduced order analysis. The order of each variable was tagged as first or zeroth order in the expanded form of Eq. (14). Then each term, or product of variables, in the equation had an order associated with it (zeroth, first, ..., up to sixth), which indicated its relative magnitude with respect to the other terms. Retaining only second-order terms and lower, along with the approximation $\Lambda_S \approx J_z$, yields the greatly simplified equation

$$T = [Qm + R/(J_z - J_1)]\Omega^2 \quad (15)$$

where

$$Q = -\sin\alpha(\epsilon_{x1}\epsilon_{x2} + \epsilon_{y1}\epsilon_{y2}) - \cos\alpha(\epsilon_{x2}\epsilon_{y1} - \epsilon_{x1}\epsilon_{y2}) \quad (16)$$

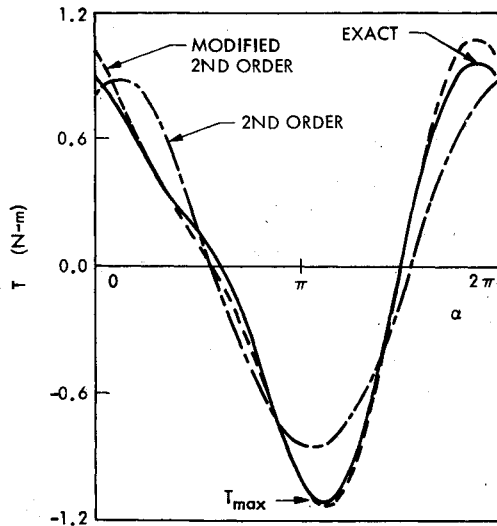


Fig. 3 Exact and approximate bearing torques as a function of α .

is the static imbalance term, and

$$R = \sin\alpha(D_{xz1}D_{xz2} + D_{yz1}D_{yz2}) + \cos\alpha(D_{xz1}D_{yz2} - D_{xz2}D_{yz1}) \quad (17)$$

is the dynamic imbalance term. Reduced mass m multiplies the static imbalance term, and the dynamic imbalance term is divided by the oblate spinning body stability term, $J_z - J_l$. The total dynamic bearing torque varies directly as the square of the spin rate ($\Omega = |H|/\Lambda_S \approx |H|/J_z$). Figure 3 compares the results of this second-order analysis to the exact solution for the Galileo mass properties listed in Table 1 (case A). The maximum bearing torque T_{\max} computed by this second-order analysis is within 22% of the correct value. It is interesting to note that small asymmetry in either body does not even contribute second-order terms to the torque equation in this analysis. Static and dynamic imbalance are the principal contributions to the dynamic bearing torque. However, static imbalance must be present on both bodies or dynamic imbalance must be present on both bodies to create the bearing torque.

The second-order analysis was then extended to the case of large asymmetry on one of the bodies. Some dual-spin spacecraft such as Galileo and DSCS-II² fall into this category. All the variables remain the same order as in the previous analysis, except that ΔJ_l and I_{xy1} (i.e., the components of S_l) are zeroth-order. Retaining only second-order terms and lower, along with the approximation $\Lambda_S \approx J_z$, yields the torque equation

$$\begin{aligned} T = & \Omega^2 \{ Qm[(J_z - J_l)^2 - S_l^2] + R[J_z - J_l] \\ & + S_l[(D_{yz2}^2 - D_{xz2}^2)\sin(2\alpha - 2\theta_1) - 2D_{yz2}D_{xz2}\cos(2\alpha - 2\theta_1) \\ & + (D_{yz1}D_{yz2} - D_{xz1}D_{xz2})\sin(\alpha + 2\theta_1) \\ & - (D_{xz1}D_{yz2} + D_{yz1}D_{yz2})\cos(\alpha - 2\theta_1)] \} \\ & \times [(J_z - J_l)^2 - S_l^2 + 2\cos(2\alpha - 2\theta_1 - 2\theta_2)S_lS_2]^{-1} \quad (18) \end{aligned}$$

where Q and R are as defined in Eqs. (16) and (17). Each set of asymmetry components ΔJ and I_{xy} has been combined into a total asymmetry term S with constant phase shift angle θ between the x axis and a principal axis of transverse moment of inertia. Figure 3 compares the results of this large asymmetry modified second-order analysis to the exact solution for the Galileo mass properties listed in Table 1 (case A). The results of the modified analysis agree much more closely with

the exact results than in the previous analysis. T_{\max} is within 2% of the correct value.

The first two terms of the resulting torque equation for the large asymmetry analysis are very similar to those obtained previously [Eq. (15)]. The additional factor multiplying Q will be very close to one, unless S_2 is also large and the magnitude of S_l approaches $J_z - J_l$; in which case the spacecraft is almost spinning unstably about its bearing axis anyway. The factor multiplying R will be very close to $1/(J_z - J_l)$, as before, unless the spacecraft is nearly unstable as discussed above. The third additional term, with S_l as the dominant factor, shows the major contribution of large asymmetry to the dynamic bearing torque. Note, however, that asymmetry on one body must couple with dynamic imbalance on the opposing body to contribute to the bearing torque.

This analysis can be extended one more step to include large asymmetry on both bodies, if desired. However, this analysis cannot be extended further to include large center of mass offsets or large xz and yz products of inertia because the assumption $\Lambda_S \approx J_z$ used in determining T will no longer be valid. The reduced order analysis could be extended to a wider variety of dual-spin spacecraft configurations if approximations for Λ_S were developed.

Application to Galileo

Further constraints must be applied to the dynamic bearing torque equations [Eq. (15) or (18)] to determine the maximum bearing torque likely to occur during the Galileo mission. These constraints depend upon the spacecraft design requirements and the operational states of the spacecraft during all phases of the mission. For Galileo, static imbalance must be within specific boundaries during the entire mission, but is not controlled during flight. Similarly, rotor and stator asymmetry are known throughout the mission. The Galileo wobble control system eliminates practically all dynamic imbalance on the rotor during most phases of the mission. However, there is one mission phase in which large dynamic imbalance is generated on the rotor. This case is discussed last.

The maximum dynamic bearing torque generated by static imbalance is found by coupling the design constraints

$$\epsilon_{x1}^2 + \epsilon_{y1}^2 \leq a^2 \quad \epsilon_{x2}^2 + \epsilon_{y2}^2 \leq b^2 \quad (19)$$

with the static imbalance term Q in Eq. (18). Allowing the maximum center of mass offsets and using the technique of Lagrange multipliers with the constraint equations to find the

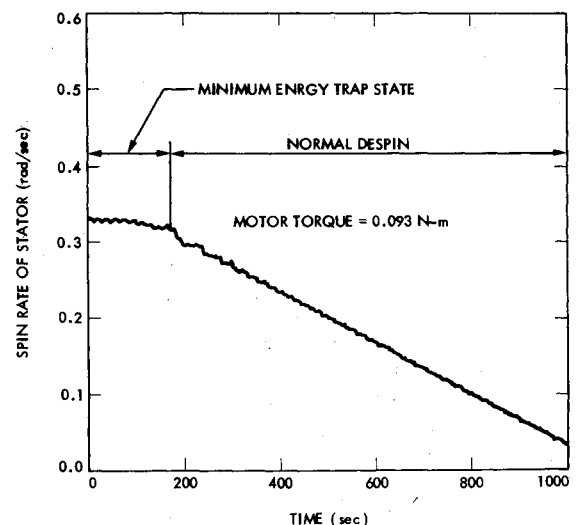


Fig. 4 Simulation run of a stator despin from 0.33 rad/s.

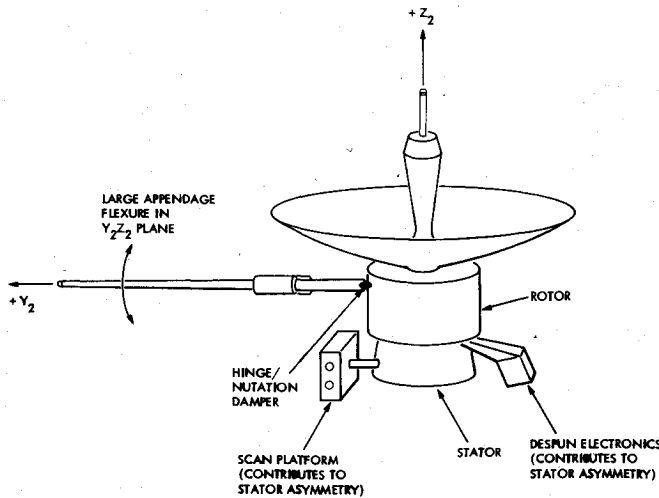


Fig. 5 Galileo dual-spin spacecraft.

maximum Q yields

$$Q_{\max} = ab \quad (20)$$

For Galileo, $a = 0.0254$ m and $b = 0.035$ m, which results in a Q_{\max} of 8.89×10^{-4} m². When the dynamic imbalance on the rotor is negligible, R is also negligible because dynamic imbalance is necessary on both bodies to contribute to bearing torque. The large asymmetry term in Eq. (18) also requires dynamic imbalance on the rotor to contribute significantly to bearing torque. Thus the maximum dynamic bearing torque for most of the Galileo mission is only dependent upon static imbalance and is given by

$$T_{\max} = Q_{\max} m \Omega^2 = 0.55 \Omega^2 \text{ N-m } (\Omega \text{ in rad/s}) \quad (21)$$

for the Galileo mass properties in Table 1 case A.

The Galileo stator is despun from 3.15 rpm (0.33 rad/s) several times during the mission. The minimum energy trap state bearing torque during despin at 3.15 rpm for the Galileo mass properties listed under case C, Table 1, (data are for an earlier configuration) is 0.318 N-m as per Eq. (15). A computer simulation of stator despin shown in Fig. 4 indicates that only 0.093 N-m or about 30% of the predicted amount of torque is required to successfully initiate stator despin for this case (but only after almost 200 s of applied torque). As the stator begins to despin, angular momentum is built up in the stator to allow it to "coast over" the maximum torque peaks.¹ This phenomenon cannot be predicted by the current analysis because the holonomic constraint $\dot{\alpha} = 0$ is violated when the stator begins to despin. However, the analysis does give an upper limit to the bearing torque.

Galileo is constructed with a large appendage attached radially to the rotor by a hinged spring-damper system such that the appendage can flex only in the y_2z_2 plane (Fig. 5). The appendage is used for passive nutation damping.⁴ As the appendage flexes, $I_{y_2z_2}$ product of inertia is generated which causes dynamic imbalance in the rotor. This dynamic imbalance is negligible except during a particular mission phase. The appendage sags substantially under the axial acceleration of a main engine burn. For large $D_{y_2z_2}$ dynamic imbalance, the

maximum torque from Eq. (18) reduces to approximately

$$T_{\max} \cong \left\{ Q_{\max} m + \frac{(J_z - J_t) [D_{y_2z_2} (\sqrt{2}/2) (D_{y_2z_1} + D_{x_2z_1})]}{(J_z - J_t)^2 - S_2^2} \right. \\ \left. + \frac{S_1 [D_{y_2z_2}^2 + \frac{1}{2} D_{y_2z_2} (D_{y_2z_1} + D_{x_2z_1})]}{(J_z - J_t)^2 - S_2^2} \right\} \quad (22)$$

for small asymmetry S_2 on the rotor and large asymmetry S_1 on the stator. For one particular worst case configuration of Galileo in which $I_{y_2z_2}$ increases by 45 kg-m² during an engine burn (case B, Table 1), the maximum dynamic bearing torque is

$$T_{\max} = \begin{array}{ccccc} (0.55 & + & 1.11 & + & 0.34) & \Omega^2 & \text{N-m} \\ \text{static} & & \text{dynamic} & & \text{asymmetry} \\ \text{imbalance} & & \text{imbalance} & & \\ = 2.00 & \Omega^2 & \text{N-m} & (\Omega \text{ in rad/s}) & \end{array} \quad (23)$$

During a large engine burn, both the rotor and stator on Galileo are spun up to 1.047 rad/s. The spin bearing motor can generate at least 2.8 N-m torque in addition to 0.5 N-m bearing friction, which can oppose the possible 2.18 N-m dynamic bearing torque created during the engine firing. This case is different from the minimum energy trap state case in that the stator must be prevented from being "wrenched" toward a minimum energy trap rather than attempting to escape one.

Conclusions

Generalization of the simple models used to study the minimum energy trap state phenomena reveals that static imbalance and dynamic imbalance are the primary contributors to trap state bearing torque. However, static imbalance or dynamic imbalance must be present on both bodies to create dynamic bearing torque. Large asymmetry on one body contributes significantly to bearing torque only if coupled with dynamic imbalance on the opposing body. Specific application of the results to the Galileo dual-spin spacecraft demonstrated techniques for prudent selection of spacecraft mass properties and the sizing of the stator despin motor.

Acknowledgments

The research described in this paper was carried out at the Jet Propulsion Laboratory, California Institute of Technology, under NASA Contract NAS7-100. The computer-assisted algebra software package MACSYMA was used to derive some of the analyses presented. MACSYMA is being developed and maintained by the Mathlab Group at MIT and is currently supported, in part, by the U.S. Energy Research and Development Administration under Contract E(11-1)-3070 and by NASA under Grant NSG 1323.

References

- ¹Scher, M.P. and Farrenkopf, R.L., "Dynamic Trap States of Dual-Spin Spacecraft," *AIAA Journal*, Vol. 12, Dec. 1974, pp. 1721-1725.
- ²Adams, G.J., "Dual-Spin Spacecraft Dynamics During Platform Spinup," *Journal of Guidance and Control*, Vol. 3, Jan.-Feb. 1980, pp. 29-36.
- ³Pringle, R.J., "On the Stability of a Body with Connected Moving Parts," *AIAA Journal*, Vol. 4, Aug. 1966, pp. 1395-1404.
- ⁴Bernard, D.E., "Passive Nutation Damping Using Large Appendages with Application to Galileo," *AIAA Paper 80-1783*, Aug. 1980.